HHS Public Access

Author manuscript

Dev Neurobiol. Author manuscript; available in PMC 2018 December 01.

Published in final edited form as:

Dev Neurobiol. 2017 December ; 77(12): 1385–1400. doi:10.1002/dneu.22544.

Sonic hedgehog antagonists reduce size and alter patterning of the frog inner ear

Sanam Zarei[1,2,3], **Kasra Zarei**[2], **Bernd Fritzsch**[1], and **Karen L. Elliott**[1,*]

[1]Department of Biology, University of Iowa, Iowa City, IA 52242, USA

[2]Department of Biomedical Engineering, University of Iowa, Iowa City, IA 52242, USA

[3]Carver College of Medicine, University of Iowa, Iowa City, IA 52242, USA

Abstract

Sonic Hedgehog (Shh) signaling plays a major role in vertebrate development, from regulation of proliferation to the patterning of various organs. In amniotes, Shh affects dorsoventral patterning in the inner ear but affects anteroposterior patterning in teleosts. Currently, it remains unknown the function of Shh in inner ear development in terms of how morphogenesis changes in the sarcopterygian/tetrapod lineage coincide with the evolution of limbs and novel auditory organs in the ear. In this study we used the tetrapod, *Xenopus laevis*, to test how increasing concentrations of the Shh signal pathway antagonist, Vismodegib, affects ear development. Vismodegib treatment dose dependently alters the development of the ear, hypaxial muscle, and indirectly the Mauthner cell through its interaction with the inner ear afferents. Together, these phenotypes have an effect on escape response. The altered Mauthner cell likely contributes to the increased time to respond to a stimulus. In addition, the increased hypaxial muscle in the trunk likely contributes to the subtle change in animal C-start flexion angle. In the ear, Vismodegib treatment results in decreasing segregation between the gravistatic sensory epithelia as the concentration of Vismodegib increases. Furthermore, at higher doses, there is a loss of the horizontal canal but no enantiomorphic transformation, as in bony fish lacking Shh. Like in amniotes, Shh signaling in frogs affects dorsoventral patterning in the ear, suggesting that auditory sensory evolution in sarcopterygians/tetrapods evolved with a shift of Shh axis specification of the ear.

INTRODUCTION

Development is a delicate balance of proliferation and topologically refined differentiation of cells. Gradients of cell signaling molecules including transcription factors are expressed at varying time frames and locations throughout the developing embryo to marshal cells into adopting and realizing appropriate specific fates (Meinhardt, 2015). One example of a diffusible signaling molecule essential for vertebrate development is Sonic Hedgehog (Shh). Shh is a morphogen that directs organogenesis, controls proliferation and differentiation, and has organizing function on the brain and limbs (Dahmane et al., 2001; Ericson et al., 1995; Merchant, 2012; Villavicencio et al., 2000; Yu et al., 2002). Mechanistically, the Shh

Corresponding author: Karen L. Elliott, Ph.D., 217 Biology Building, The University of Iowa, Iowa City, IA 52242, karen-elliott@uiowa.edu, Phone: (319) 335-1089.

pathway employs primarily two transmembrane proteins – Patched (Ptc) and Smoothened (Smo) (Sharpe et al., 2015). Shh binds to the twelve-pass transmembrane protein Ptc (Murone et al., 1999). Without Shh, Patched forms a complex with a seven-pass transmembrane protein, Smo (Chen and Struhl, 1998; Dahmane et al., 2001; Murone et al., 1999). Once Shh binds to Ptc, Smo is released, becomes phosphorylated, and activates the downstream signaling cascade (Chen and Struhl, 1998; Murone et al., 1999). Downstream signaling is predominantly mediated by the zinc-finger transcription factors Gli1-3 regulating the expression of target genes (Huangfu and Anderson, 2006; Jacob and Briscoe, 2003). The *Xenopus* Smo protein is slightly shorter (787 amino acids versus 695 amino acids), but shares the Frizzled/Smoothened membrane region as well as the seven transmembrane receptor domain with mammalian Smo. Smo is highly conserved across bilateria and so is the Hedgehog signaling pathway.

Elimination or reduction of Shh signaling has been demonstrated to adversely affect proliferation, differentiation, and morphogenesis in normal ear development (Bok et al., 2005; Bok et al., 2007; Groves and Fekete, 2012; Hammond et al., 2003; Koebernick et al., 2003; Liu et al., 2002; Riccomagno et al., 2002; Riccomagno et al., 2005; Whitfield and Hammond, 2007; Wu and Kelley, 2012). However, the specific effects on inner ear morphogenesis are not consistent across species. In mice and chickens, absence of Shh signaling results in dorsoventral patterning defects, whereas in zebrafish, it results in anteroposterior patterning defects (Groves and Fekete, 2012; Whitfield and Hammond, 2007; Wu and Kelley, 2012). In mice and chickens, loss of Shh signaling, either directly or indirectly through downstream signaling molecules, such as Gli3, results in the absence of the cochlea/basilar papilla and the horizontal canal (Bok et al., 2005; Bok et al., 2007; Liu et al., 2002; Riccomagno et al., 2002). In contrast in zebrafish, loss of Shh signaling through mutation of the Smo receptor resulted in the formation of ears with two mirror-image anterior halves, whereas overexpression of Shh resulted in ears with two mirror-image posterior halves (Hammond et al., 2003) comparable to enantiomorphic ears in amphibians after anteroposterior axis reversal (Fritzsch et al., 1998; Harrison, 1945; Waldman et al., 2007; Yntema, 1948). Thus, enantiomorph ears as in zebrafish can be experimentally induced in amphibians but have not been reported in amniotes following Shh signal manipulation. To date, the role for Shh in inner ear morphogenesis has not been determined for frogs, a line of tetrapods that have a basilar papilla in their ear (Fritzsch et al., 2013). Given the ability of frogs to form mirror-image twin ears (Waldman et al., 2007), it is possible that, like zebrafish, Shh functions to pattern the anteroposterior axis of the ear. However, since frogs are tetrapods with a basilar papilla, it is equally likely that Shh functions to pattern the dorsoventral axis of the ear, much like in mice and chicken. In contrast to all Shh null mutations reported thus far, the effect of the Smo antagonist cyclopamine has been claimed to enlarge ears in *Xenopus laevis* and overexpression of a Shh signaling antagonist, hedgehog interacting protein, resulted in the formation of extra ears (Koebernick et al., 2003). However, the specific effect on inner ear morphogenesis related to ear patterning and in particular basilar papilla development was not reported in that study. Since in mice, chickens, and zebrafish, reduction in Shh signaling results in smaller ears, albeit with a different polarity, this incongruent finding in *Xenopus* may suggest frogs react to Shh inhibition differently than other vertebrates, possibly including

axis effects. In this context, a more recent paper on *Xenopus* malformations induced with cyclopamine did not specifically suggest formation of enlarged ear vesicles and mentioned no axis defects either (Martin et al., 2007). Given this limited information and incongruent information on Shh signaling on inner ear patterning and considering the possible evolutionary significance of auditory organ development in amniotes and its absence following loss of Shh signaling, determining the role of Shh signaling on inner ear development and patterning in frogs could provide insights into the evolution of auditory epithelia in sarcopterygians/tetrapods (Fritzsch et al., 2013) through altered developmental patterning of the inner ear by Shh.

The goal of this study is to understand how graded reduction in Shh signaling via treatment with a more specific Smo antagonist, Vismodegib (Rudin, 2012), affects patterning of the inner ear in the frog, *Xenopus laevis*. Vismodegib (GDC-0449) is an orally active Hedgehog pathway inhibitor with an IC_{50} of 3 nM that also inhibits P-gp and ABCG2 with IC_{50} values of 3.0 μM and 1.4 μM, respectively. Vismodegib has been used in clinical trials and model organisms to antagonize the Shh/Smo induced hyperproliferation of tumors such as medulloblastoma (LoRusso et al., 2011; Morinello et al., 2014; Rudin, 2012; Shimizu et al., 2015). Given the conservation of Shh/Smo pathway in bilateria, this Smo antagonist will likely affect the Shh pathway in *Xenopus*, but details of drug interactions remain unknown. Using a uniform and graded disruption of the Shh-Smo pathway, we want to determine whether Shh plays a role in dorsoventral or anteroposterior patterning in the amphibian, and, by logical inference in the ancestral tetrapod ear. Specifically, we would like to find out if progressively reduced Shh signaling leads to enantiomorphic twin ears as in zebrafish or reduced sensory epithelia formation such as horizontal canal crista as in mice and chicken. In addition, we will investigate general phenotypic changes following treatment of Vismodegib, such as effects on olfactory, eye, hypaxial muscle, and brain development. Finally, using a newly developed imaging apparatus (Zarei et al., 2017), we report how mild phenotypic changes affect the swimming behavior of the tadpole, presumably through affecting the inner ear/Mauthner cell interactions mediating the fast escape response. These insights will guide follow up work assessing how disrupted ear development affects swimming behavior after grafting Vismodegib-treated ears onto control *Xenopus* (Elliott et al., 2015a; Elliott et al., 2015b)

METHODS

Ethics Statement on Use of Animals

All protocols involving the collection and use of animals was granted approval by the University of Iowa Institutional Animal Care and Use Committee (IACUC; #1303056). All experiments were performed in accordance to the IACUC's guidelines for the use of laboratory animals.

Animals

Xenopus laevis female frogs were induced to ovulate via an injection of human chorionic gonadotropin and the resulting oocytes were collected for experimental use. Oocytes were fertilized in a sperm suspension in 0.3X Marc's Modified Ringer's (MMR) solution. Treated

(see below) and untreated embryos were kept at 15 – 18 °C in 30 mm Petri dishes containing 0.1X MMR until they reached stage 46 (Nieuwkoop and Faber, 1956). Once they reached stage 46, a few animals were randomly selected for a behavioral analysis (see below). Following the analysis, those animals and all other animals were anesthetized in 0.2% Benzocaine and fixed in 4% paraformaldehyde (PFA).

Treatment with Vismodegib

A 1 mM stock solution of Vismodegib (MedChem Express; catalog # HY-10440) was made in DMSO. Once the embryos were confirmed to be undergoing gastrulation (Koebernick et al., 2003), twenty embryos each were treated with 6.25 μM, 12.5 μM, 18.75 μM, and 21.875 μM Vismodegib. An additional group of twenty was left untreated (control animals). Each group was kept at 15 – 18 °C in 30 mm Petri dishes until they reached stage 46 (Nieuwkoop and Faber, 1956). The Vismodegib solution was replaced daily to ensure consistency of the chosen concentration over time. This interval is consistent with Vismodegib's half-life, which is suggested to be 14 hours in humans and over two days of constant plasma levels (Rudin, 2012). What the exact concentration of IC_{50} is for Xenopus Smo proteins is unknown.

Behavioral Experiments

A total of seventeen tadpoles (seven controls and ten animals treated with 6.25 μM Vismodegib) were used to study the effect of Shh inhibition on the escape behavior. Individual tadpoles were transferred to an experimental chamber to perform movement pattern analysis, as described (Zarei et al., 2017), and were allowed to adapt for approximately ten minutes before testing. The imaging apparatus uses a high-speed camera to obtain real-time, high-resolution images of tadpole movements, recorded in a temperature-controlled test chamber following mechanical stimulation with a solenoid actuator, to elicit a C-start response. This response is driven by the Mauthner cells, two large reticulospinal neurons in the hindbrain of aquatic vertebrates such as *Xenopus laevis* (Korn and Faber, 2005). The Mauthner cells receive input from inner ear afferents through the lateral dendrites and projects contralaterally down the spinal cord to synapse on spinal motor neurons to promote contraction of muscles that permit movement away from a stimulus (Elliott et al., 2015a). Ventral images of the tadpoles were recorded at 400 frames per second and at a spatial resolution of 1024×1024 pixels. Each of the seven control and ten treated animals underwent a total of four trials each. Following the completion of each trial, each animal was allowed to recover for a minimum of three to five minutes prior to the start of the subsequent trial. Response time was determined as previously described (Zarei et al., 2017) and means were compared using a two-sample t-test assuming unequal variances.

Analysis of Swimming Behavior

Following image acquisition, image montages for each trial were constructed consisting of the tadpole's movement in the first 2.5 ms following application of the stimulus for each of the four trials. C-start response times for each behavioral sequence and flexion angles for each still frame were quantified using the same manual grading system defined in K. Zarei et al. (2017). The maximum flexion angle, as measured from each animal's tail to the tip of the nose, was then identified for each trial.

Phenotypic Assessment

Images were obtained for each animal using a Leica dissecting microscope to document phenotypes. Using the images from the dissecting microscope, each animal was scored using the following categories:

1. otoconia development: a) two distinct otoconia, b) fusion of otoconia, and c) no otoconia development;
2. olfactory system development: a) segregated olfactory system, b) partially fused olfactory system, and c) completely fused olfactory system;
3. tail development: a) normal, straight tail structure b) kinked tail.
4. eye development: a) normal pigmentation, b) 1/4 of pigmentation missing, c) 1/2 of pigmentation missing, and d) 3/4 of pigmentation missing.

Dextran Amine Labelling

Animals that had reached stage 46 were anesthetized by immersion in 0.2% Benzocaine. To label all ventral and lateral dendrites emerging from the Mauthner cells, the spinal cord of each animal was bisected just caudal to the hindbrain-spinal cord junction and a small amount of Texas Red 3000 MW dextran amine dye was inserted into the point of bisection using a tungsten needle (Fritzsch, 1993). Following the procedure, all animals were transferred to 0.1 × MMR for 3 hours in order to promote dye diffusion into the hindbrain. At the conclusion of at least 3 hours, animals were fixed in 4% PFA.

Immunohistochemistry

Fixed embryos were skinned and then immunostained with an antibody against acetylated tubulin (Fariñas et al., 2001) to label all nerves and myosin (Myo) VI to label all inner ear hair cells and muscle fibers of somitic origin (Kaiser et al., 2008). In addition, brains were removed from embryos and immunostained with 3A10 antibody to label the Mauthner cells (Liu et al., 2003; Pattern et al., 2007). The concentration used for acetylated tubulin (Cell Signaling Technology) was 1:800, for Myo VI (Proteus Biosciences) was 1:400, and for 3A10 (Developmental Studies Hybridoma Bank, University of Iowa) was 1:125. Species-specific fluorescently labelled secondary antibodies (Alexa) were used at a concentration of 1:500. In addition, embryos were stained with Hoechst stain. Embryos were mounted dorsal side up on a slide in glycerol. For some embryos, 100 μm sections were taken of embryos imbedded in 3% agarose using a VF-700 microtome and were mounted on a slide in glycerol. Brains were mounted ventral side up. Image stacks were acquired at 3 μm and 6 μm intervals with a Leica TCS SP5 confocal microscope.

Measuring Ear Dimensions Using Hoechst Staining

The dimensions of each ear were determined from Hoechst-stained embryos using the Leica software. Confocal z-series images were examined individually to determine the maximum length along the anteroposterior axis, the maximum width along the mediolateral axis, and the maximum height along the dorsoventral axis (Fig. 2B and 2C). Maximum height along the dorsoventral axis was calculated by multiplying the number of images required to image

the entire ear by the distance between images. The measurements from both ears were averaged to give one value per embryo.

Three-Dimensional Reconstruction of Ear Sensory Epithelia and Mauthner Cells

Confocal images of immunohistochemically-labeled embryos and brains were used for three - dimensional (3D) reconstruction of inner ear sensory epithelia and Mauthner cells (Kopecky et al., 2012). In order to reconstruct the ear sensory epithelia, confocal image Z - series stacks of embryo heads were loaded into Amira Version 5.4 software for manual segmentation (Kopecky et al., 2012). The Amira software was used to generate the 3D reconstructions of the individual hair cells in the sensory epithelia of the ear (utricular macula, saccular macula, lagenar macula, anterior canal crista, horizontal canal crista, and posterior canal crista). For each embryo, the total number of distinct sensory epithelia from the 3D reconstructions of the individual hair cells in the sensory epithelia of the inner ear were counted taking note of the identity of specific sensory epithelia that had fused with one another or had failed to segregate.

For the three-dimensional reconstruction of Mauthner cells, the brains of embryos implanted with Texas Red 3000 MW dextran amine into the spinal cord were removed and mounted ventral-side up in glycerol on a microscope slide. Confocal Z-series images at 1.5 μm were taken of the hindbrain using a Leica TCS SP5 confocal microscope. Z-series stacks were loaded into Amira Version 5.4 software for manual segmentation as described previously (Kopecky et al., 2012). From the 3D reconstructed Mauthner cells, the total number of terminal branches of the lateral dendrite of each Mauthner cell were counted.

Statistical Analysis

A Type 3 Test of Fixed Effects was used to determine significance for the averaged ear measurement lengths along the anteroposterior, mediolateral and dorsoventral axes within each animal. A one-way ANOVA was conducted to compare the mean differences of the averaged ear measurement lengths along both the anteroposterior, mediolateral, and dorsoventral axes among the five groups (control, 6.25 μM, 12.5 μM, 18.75 μM, and 21.875 μM Vismodegib). A two-sample t test assuming unequal variances was used to determine significance for all terminal branch count analyses.

For the behavioral analysis, the calculated response time and angle at maximal flexion from the four trials for each animal were averaged to generate a distinct value for each animal. A two-sample t test assuming unequal variances was used to compare the averaged response time and angle of maximal flexion values between control and treated animals. All statistical tests were evaluated for significance at the 0.05 significance level. Data are presented as mean ± SEM unless indicated otherwise.

RESULTS

Phenotypic Assessment of Animals on various organ developments

Prior to assessing the effect of Vismodegib treatment on the inner ear, we assessed the phenotypic changes across the animal at varying doses. This would allow us to interpret our

findings on the ear as being specific, or potentially due to more systemic alterations (ear specific versus systemic effects compounding ear specific effects). Under our assay conditions, 25 μM of Vismodegib was found to be lethal in *Xenopus*, and thus we analyzed only lower concentrations of the drug. It should be noted that all our concentrations 6.25 – 21.875 μM are in the range of reported plasma concentrations in humans after Vismodegib treatment [22 μM (Rudin, 2012)]. It should be noted that Vismodegib in humans and frogs is in the same range of effective concentration but clearly above the IC_{50} measured in isolated Smo proteins.

Olfactory—Reduction of Shh signaling through treatment with varying concentrations of Vismodegib resulted in a dose-dependent effect on phenotypic changes in tadpoles assessed at stage 46 (Fig. 1A – D). While control animals display two distinct olfactory groves (Fig. 1A'), there was a tendency towards complete fusion of the two olfactory groves as a function of increasing Vismodegib concentration (Figs. 1A" and 1A"'). Animals treated with 6.25 μM Vismodegib exhibited partially fused olfactory epithelia (Fig. 1A"). While partial olfactory fusion was the dominant phenotype in animals treated with 12.5 μM Vismodegib (Fig. 1A"), there was complete fusion in a few animals (Fig. 1A"'). By 18.75 μM of Vismodegib, all animals exhibited complete fusion of the olfactory epithelia resulting in monorhinic animals (Fig. 1A"').

Otoconia—Aberrations in otoconia development were also evident with Vismodegib treatment (Fig. 1B). Compared to control animals that had two distinct otoconia masses associated with the utricle and saccule (Fig. 1B'), some animals treated with 6.25 μM Vismodegib had a single otoconia mass (Fig. 1B"). This trend of reduction in otoconia masses increased with animals treated with 12.5 μM and 18.75 μM Vismodegib. Animals treated with 21.875 μM lacked otoconia formation altogether (Fig. 1B"'), indicating deficits in otoconia development with reduced Shh signaling in *Xenopus*. This is in line with similar observations in other animals after Shh signaling manipulation (Forristall et al., 2014; Hammond et al., 2003).

Eyes—Eye pigmentation was also affected following treatment with Vismodegib (Fig. 1C). As with control animals, nearly all animals treated with 6.25 μM Vismodegib exhibited full eye pigmentation (Fig. 1C'). A few animals treated with 6.25 μM Vismodegib, over half of animals treated with 12.5 μM Vismodegib, and just a few animals treated with 18.75 μM and 21.875 μM Vismodegib lost eye pigmentation in the most ventral part of the eye (Fig. 1C"). Approximately half of animals treated with 18.75 μM and 21.875 μM Vismodegib lost eye pigment in half of the eye [Fig. 1C"']. Finally, in a few animals treated with 18.75 μM Vismodegib and in just under half of the animals treated with 21.875 μM Vismodegib, eye pigment was nearly absent (Fig. 1C"").

Tail—In addition, tail development was affected as a result of Vismodegib treatment (Figure 1D). Approximately two-thirds of animals treated with 6.25 μM Vismodegib exhibited a kink in the caudal portion of their tails, whereas all to nearly all animals treated with 12.5 μM, 18.75 μM, and 21.875 μM Vismodegib exhibited a kinked tail (Fig. 1D") compared to

the straight tail of control animals (Fig. 1D'). These data indicate that there is an effect of the concentration of Shh signaling on tail development.

In conclusion, our dose dependent morphogenetic defects are in line with more limited data reported on rat embryos (Morinello et al., 2014) and indicate that Vismodegib is a potent teratogen that should not be given at early human pregnancies as typical concentrations are in the same range as the ones used here in frogs.

Effect of Vismodegib on Ear Size

Since a previous study using the Smo antagonist, cyclopamine, demonstrated enlarged ears (Koebernick et al., 2003), we next examined the inner ear dimensions (Fig. 2B–C). In contrast to the reported data with cyclopamine treatment, treatment with Vismodegib resulted in a dose-dependent reduction in ear dimensions analyzed along both the anteroposterior, dorsoventral and mediolateral axes (Fig. 2A). This decrease in ear size was more profound along the anteroposterior dimension of the ear compared to the mediolateral and dorsoventral dimension of the ear. While ears from animals treated with 12.5 μM and greater doses of Vismodegib were significantly reduced in length along the anteroposterior axis from controls, only 18.75 μM and 21.875 μM Vismodegib-treated animals were significantly reduced along the mediolateral axis from controls (Fig. 2A). Furthermore, the reduction in length along the anteroposterior axis at the highest dose of Vismodegib was approximately 2-fold, whereas along the mediolateral axis, it was only approximately 1.3-fold. While the ears were reduced in size along the dorsoventral axis as the dose of Vismodegib increased (Fig. 2A), it was not a significant reduction; however, when all three measurements were used to calculate the approximate volume of the ear, there was a significant reduction in volume as the dose of Vismodegib increased (Fig. 2D). The reduction in ear size correlates well with the reduced proliferation in various tumors that are stimulated by the Shh/Smo pathway (LoRusso et al., 2011; Yauch et al., 2009) and is in agreement with the role of Smo in proliferation regulation through activation of n-Myc in both medulloblasotma (Yang et al., 2008) and ear development (Kopecky et al., 2011).

Effect of Vismodegib on Sensory Epithelia Development

To fully characterize the degree of sensory epithelia development following treatment with Vismodegib, individual hair cells were labeled with antibody against MyoVI (Fig. 3B) and were then subsequently 3D reconstructed (Figs. 3C–3G'). Animals treated with Vismodegib exhibited a dose-dependent reduction in sensory epithelia development (Fig. 3A). Compared with six distinct sensory epithelia in control animals (Fig. 3A, 3B, and 3C), animals treated with 6.25 μM or 12.5 μM Vismodegib exhibited four to five distinct sensory epithelia (Figs. 3D, 3D', and 3E) whereas animals treated with 18.75 μM and 21.875 μM Vismodegib exhibited between two to four distinct sensory epithelia (Figs. 3F and 3G). Some of the reductions in the number of distinct epithelia likely resulted from incomplete segregation of linear acceleration-detecting epithelia [utricle, saccule, and lagena; (Fritzsch et al., 2002)] due to downregulation of proliferation related to reduced n-Myc activity [(Kopecky et al., 2011) (Table 1)]. While sometimes somewhat ambiguous in terms of clear-cut segregation, the trend towards variable fusion/lack of segregation was nevertheless clear (Fig. 3).

The most common sensory epithelia phenotype following Vismodegib treatment was the formation of what appeared to be a single, fused saccule-lagena epithelium. With the exception of one ear from one animal treated with 12.5 μM Vismodegib, all animals across all doses displayed some lack of segregation of the saccule and lagena. At 12.5 μM Vismodegib, about one-third of the ears showed some formation of a single utricle-saccule-lagena epithelium, which increased to over 80 percent at 18.75 μM Vismodegib. By 21.875 μM Vismodegib, most animals had a single utricle-saccule-lagena epithelium. Sensory epithelial patches were sometimes connected by a few hair cells in a “bridge” (Fig. 3F, note the bridge of hair cells connecting the saccule and lagena) or formed a single confluent epithelium (Fig. 3G, 3G’) comparable to cyclostome macula communis (Fritzsch et al., 2013). In contrast, defects in the angular acceleration-detecting sensory epithelia were not as frequent. Consistent with n-Myc mutants (Kopecky et al., 2011), of the 3 semicircular canal cristae, the horizontal canal crista was most often absent following Vismodegib treatment. Even following treatment with 6.25 μM or 12.5 μM of Vismodegib, one to two ears were lacking the horizontal canal crista. Following treatment with 18.75 μM or 21.875 μM of Vismodegib, slightly more than half of the ears lacked a horizontal canal crista, and in a few instances, the anterior canal crista was also absent as a distinct epithelium in these animals. At all doses of Vismodegib, the posterior canal was always present and in one ear treated with 12.5 μM Vismodegib, there were two posterior canal cristae or possibly two widely spaced hemicristae.

Effect of Vismodegib on Hypaxial Muscle

Since our data following Vismodegib treatment did not agree with data presented following cyclopamine treatment (Koebernick et al., 2003), and knowing that cyclopamine treatment has been shown to expand hypaxial muscle (Martin et al., 2007), we examined hypaxial muscle formation following Vismodegib treatment, a more potent and specific Smo antagonist (LoRusso et al., 2011; Rudin, 2012). Reducing Shh signaling through Vismodegib treatment in *Xenopus* results in a significant rostral expansion of hypaxial muscle fibers (Fig. 4), as previously described for cyclopamine (Martin et al., 2007). In animals treated with 6.25 μM Vismodegib, the rostral boundary of the hypaxial muscle extended 223 ± 18 μm past the anteroposterior midline of the ear, near the rostral limit of the notochord, whereas in control animals, the rostral boundary of the hypaxial muscle was 78 ± 15 μm caudal to the anterior-posterior midline of the ear (Fig. 4A and 4B). Importantly, and expanding to previous observations on this phenomenon after cyclopamine treatment, we found that these muscle fibers expanded rostrally between the brain and the ear (Fig. 4C). While muscle fibers are thus adjacent to hair cells and could possibly receive inner ear efferents as demonstrated for other motor neurons projecting to ears (Elliott et al., 2013; Fritzsch and Elliott, 2017) we could trace all innervation to post-otic efferents, suggesting the anterior translocation of muscle fibers is accompanied by translocating the innervation instead of receiving new innervation from inner ear efferents of facial branchial motoneurons.

Effect of Vismodegib Treatment on Mauthner Cell Formation

Given that physical ear removal can negatively affect the development of the Mauthner cell and its lateral dendrites (Elliott et al., 2015a), we investigated whether our reduced ears

following Vismodegib treatment had any effect on the development of the Mauthner cell itself and/or of its lateral dendrites. The Mauthner cell was always present in animals treated with varying concentrations of Vismodegib (Fig. 5A, 5B). The number of lateral dendrite branches was significantly reduced from controls at the 6.25 μM dose of Vismodegib (Fig. 5C, 5D, 5E). Furthermore, in animals treated with 6.25 μM, there is an approximately two-fold reduction in the diameter of the Mauthner cell axon when compared with control animals (Fig. 5F).

Effect of Vismodegib Treatment on Swimming Behavior

Since Vismodegib treatment negatively affected ear and Mauthner cell development and positively affected hypaxial muscle development, and since vestibular input and muscle output are involved in swimming and are coordinated through the Mauthner cell, we evaluated if there was an effect on the swimming behavior of the animals. Given that the possession of a kinked tail would add an additional variable, only animals with straight tails were selected (n = 10 animals treated with 6.25 μM Vismodegib). Animals were placed in a swimming chamber over a high-speed camera and stimulated with a forceful tap (Fig. 6A). Animals treated with 6.25 μM Vismodegib require 28.5 milliseconds to initiate the C-startle response following stimulation, which is a significantly longer delay than the 24 milliseconds necessary for control animals to elicit a response (Figs. 6B, 6C, and 6D), indicating that the reduced ears and Mauthner cell alterations negatively affected the speed of the escape response. Vismodegib treatment affected the angle of the C-start at maximum flexion (Fig. 6E), though not at a statistically significant level. In animals treated with 6.25 μM Vismodegib, the head-to-tail angle at maximal flexion is 45.9 degrees, which results in the animals assuming a tighter, U-shaped like configuration (Fig. 5C) as compared with the C-shaped configuration of controls, which have a 56.0 degree angle (Fig. 5B). This suggests that the phenotypic changes, and most likely the expansion of hypaxial muscle into the head, following Vismodegib treatment affects the shape of the behavioral response. Detailed correlation of muscle shift with the angle of flexion in more animals is needed to consolidate this observation.

DISCUSSION

The present study analyzes how the Shh/Smo antagonist, Vismodegib, affects development of the inner ear, musculature, and Mauthner cell coupled with quantitative characterization of deficits in motor control and vestibular functioning in the frog, *Xenopus laevis*. Our data reject some previous observations on ear development using a less specific Smo antagonist, cyclopamine (Koebernick et al., 2003) but confirm observations on anterior translocation of hypaxial muscle fibers (Martin et al., 2007). Our data on ear size reduction and fusion of sensory epithelia are consistent with Shh function in proliferation regulation through n-Myc (Kopecky et al., 2011; Yang et al., 2008) leading to tumor formation (Morinello et al., 2014; Rudin, 2012; Shimizu et al., 2015) and show that Shh affects the size of the ear.

Aberrant Development and Morphogenesis in Embryos Treated with Vismodegib

The defects in the olfactory system, eye, ear, and the tail following treatment with the Smo antagonist, Vismodegib, indicate that Shh plays a role in their development and is a potential

teratogen (Morinello et al., 2014). Previous data has shown that Shh plays a role in olfactory development (Belloni et al., 1996) and that inhibition of Shh signaling through the Smo antagonist, cyclopamine, results in a reduced olfactory epithelia (Nagase et al., 2005). Our data on olfactory epithelia fusion following Vismodegib treatment is congruent with this finding. In addition to olfactory defects, defects in eye formation has been associated with Shh signaling disruption by cyclopamine (Incardona et al., 1998) and its effect on the Shh pathway (Amato et al., 2004). Our incomplete fusion of eyes even in the highest concentration of Vismodegib suggest that cyclopamine may affect additional pathways as it seems to have a more effective fusion effect on eyes compared to Vismodegib. Kinked tails can arise from multiple pathways and establishing causality of Vismodegib in this defect is beyond the scope of this paper.

Aberrant Ear Development in Embryos Treated with Vismodegib

We demonstrate decreasing ear size, decreasing numbers of sensory eptihelia and reduction in otoconia with increasing dose of Vismodegib. While Hammond et al. (2003) reports alterations with otoconia formation, they do not report a complete loss of otoconia with their Smo mutants. In Hammond et al., (2003) the posterior otoconia resembles that of the anterior otoconia in Smo mutants and both sit over a single, ventral/anterior-like sensory epithelia. While there is no direct link known between Shh signaling and otoconia formation, there are links between proteins secreted from hair cells, for example Otopetrin-1 (Hurle et al., 2003), and otoconia formation. Perhaps then the reduction in otoconia formation is, in part, a result of having fewer distinct sensory epithelia of the inner ear that may affect their distinct development (Nichols et al., 2008). However, the reason for the complete absence of otoconia in two of our cases despite the presence of sensory epithelia after Vismodegib treatment is unknown. Together these results show the extent that the various doses of Vismodegib have on the embryo as a whole. The lower concentrations of Vismodegib had minimal effect on the total body phenotypes. Thus, it is likely, especially at these lower concentrations of Vismodegib, that the effect on the ear is specific, rather than secondary.

Previous studies in *Shh*$^{-/-}$ mice, demonstrated inner ear epithelia defects, specifically loss of the lateral/horizontal canal, of the utricular and saccular chambers, and of the entire cochlear duct (Liu et al., 2002; Riccomagno et al., 2002). Likewise, loss of one of the downstream signaling molecules, Gli3 (Bok et al., 2007), affected dorsoventral patterning in chicken and mice, including loss of the cochlea and horizontal canal. The horizontal canal crista depends on Foxg1 (Pauley et al., 2006) and n-Myc mediated proliferation (Kopecky et al., 2011). Importantly, the posterior canal crista always remained as a discrete sensory epithelium easily identifiable based on its unique fiber supply (Fritzsch et al., 2013). In contrast, previous studies in zebrafish demonstrated that loss of Shh signaling affects anteroposterior patterning, resulting in a mirror duplication of the anterior half of the ear at the expense of the posterior saccule (Hammond et al., 2003). In addition, in zebrafish, the horizontal canal was always present (Hammond et al., 2003). Consistent with the reports in mice mutant for Shh signaling (Bok et al., 2005; Bok et al., 2007; Riccomagno et al., 2002; Riccomagno et al., 2005), we show here that a reduction in Shh signaling via treatment with Vismodegib results in incompletely differentiated ears in *Xenopus*. In particular, at higher doses of

Vismodegib, all animals have an unsegregated utricle, saccule, and lagena comparable to the macula communis found in cylostomes (Fritzsch et al., 2013; Lewis et al., 1985). The loss of a horizontal canal crista is in line with Shh/Smo regulation of n-Myc that regulates proliferation in medulloblastoma (Heretsch et al., 2010; Yang et al., 2008; Yauch et al., 2009). Loss of n-Myc results in the loss of the horizontal canal and its crista (Kopecky et al., 2011). Our data are in line with a role of Shh/Smo in proliferation regulation.

Importantly, anteroposterior mirror-image ears (enantiomorphic ears) were never observed in our study, suggesting that bony fish anteroposterior patterning defects using Shh (Hammond et al., 2003; Whitfield and Hammond, 2007) is possible unique to these vertebrates. Overexpression of Shh signaling through constitutively active Smo or other means (Hyman et al., 2009) in lampreys is now needed to evaluate how increased growth and segregation of the common macula leads to various distinct sensory epithelia in lampreys and may affect the unusually symmetric hagfish ear (Fritzsch et al., 2002; Lewis et al., 1985). Alteration in Shh signaling in the tetrapod lineage could be linked to epithelial multiplication in tetrapods (Fritzsch and Wake, 1988), including possibly the formation of a novel auditory sensory epithelium in the sarcopterygian lineage (Fritzsch, 1987; Fritzsch et al., 2013)

In contrast to the finding by Koebernick et al. (2003) using the Smo antagonist, cyclopamine, we did not see enlarged inner ears with treatment with the Smo antagonist, Vismodegib. In fact, in our study, increasing concentrations of Vismodegib resulted in a dose-dependent decrease in both the anteroposterior and mediolateral lengths of the inner ear. This suggests that Vismodegib and cyclopamine, while both are reported to be Smo antagonists, may likely have different specificities and/or cyclopamine may have off target effects that can affect ear development. Given that cyclopamine has in IC_{50} of 46nM (Peukert et al., 2009), whereas Vismodegib has an IC_{50} of only 3nM (Scales and de Sauvage, 2009), it would seem likely that the higher dose of cyclopamine needed and used may have caused secondary effects in ear development possibly through its interactions with other nearby developing systems.

Vismodegib Treatment Results in Aberrations in Swimming Behavior

Treatment with Vismodegib resulted in animals displaying a delayed C-start response compared to those of control animals. Mauthner cells are responsible for initiating the C-start reflex (Korn and Faber, 2005). Size of the dendritic tree is directly proportional to the inner ear input (Elliott et al., 2015a; Goodman and Model, 1988; Piatt, 1969) possibly affecting the speed at which an action potential can be generated. In addition, the speed at which an action potential travels along the axon is directly related to the diameter of the axon (Hartline and Colman, 2007). Cyclopamine treatment negatively affected commissural neurons (Charron et al., 2003), but there was no apparent effect on axon crossing at the midline by Mauthner cells in animals treated with 6.25 μM Vismodegib. The reduced dendrites and soma size can possibly explain the axon diameter changes of the Mauthner cell.

In summary, our data show that Vismodegib has teratogenic effects on multiple organ developments, including the ear and associated brainstem resulting in altered startle responses. The ear shows a dose-dependent reduction in size and epithelial segregation

consistent with effects reported in amniotes but not in bony fish. Reducing a developing tetrapod ear to a lamprey like ear using Vismodegib offers a novel test for functional assessment of reduced ears in combination with our established transplantation and behavioral test system (Elliott et al., 2015a; Zarei et al., 2017)

Acknowledgments

This material is based upon work supported by the NASA Iowa Space Grant Consortium under Grant No. NNX10AK63H. SZ and KZ were supported by Iowa Space Grant Consortium (ISGC) scholarships. KE is supported by an NIH R03 (DC015333). The use of the Leica TCS SP5 multi-photon confocal microscope was made possible by a grant from the Roy. J. Carver Charitable Trust. The monoclonal antibody 3A10, developed by Jessell, TM, Dodd, J, and Brenner-Morton, S, was obtained from the Developmental Studies Hybridoma Bank (DSHB), developed under the auspices of the NICHD and maintained by The University of Iowa, Department of Biology, Iowa City, IA 52242. We also thank the Office of the Vice President for Research (OVPR) of the University of Iowa for support. The authors have no conflicts of interest to declare.

References

Amato M, Boy S, Perron M. Hedgehog signaling in vertebrate eye development: a growing puzzle. Cellular and Molecular Life Sciences CMLS. 2004; 61:899–910. [PubMed: 15095011]

Belloni E, Muenke M, Roessler E, Traverse G, Siegel-Bartelt J, Frumkin A, Mitchell HF, Donis-Keller H, Helms C, Hing AV, Heng HHQ, Koop B, Martindale D, Rommens JM, Tsui LC, Scherer SW. Identification of Sonic hedgehog as a candidate gene responsible for holoprosencephaly. Nat Genet. 1996; 14:353–356. [PubMed: 8896571]

Bok J, Bronner-Fraser M, Wu DK. Role of the hindbrain in dorsoventral but not anteroposterior axial specification of the inner ear. Development. 2005; 132:2115–2124. [PubMed: 15788455]

Bok J, Dolson DK, Hill P, Rüther U, Epstein DJ, Wu DK. Opposing gradients of Gli repressor and activators mediate Shh signaling along the dorsoventral axis of the inner ear. Development. 2007; 134:1713–1722. [PubMed: 17395647]

Charron F, Stein E, Jeong J, McMahon AP, Tessier-Lavigne M. The Morphogen Sonic Hedgehog Is an Axonal Chemoattractant that Collaborates with Netrin-1 in Midline Axon Guidance. Cell. 2003; 113:11–23. [PubMed: 12679031]

Chen Y, Struhl G. In vivo evidence that Patched and Smoothened constitute distinct binding and transducing components of a Hedgehog receptor complex. Development. 1998; 125:4943–4948. [PubMed: 9811578]

Dahmane N, Sánchez P, Gitton Y, Palma V, Sun T, Beyna M, Weiner H, i Altaba AR. The Sonic Hedgehog-Gli pathway regulates dorsal brain growth and tumorigenesis. Development. 2001; 128:5201–5212. [PubMed: 11748155]

Elliott KL, Houston DW, DeCook R, Fritzsch B. Ear manipulations reveal a critical period for survival and dendritic development at the single-cell level in Mauthner neurons. Developmental Neurobiology. 2015a; 75:1139–1351.

Elliott KL, Houston DW, Fritzsch B. Transplantation of Xenopus laevis tissues to determine the ability of motor neurons to acquire a novel target. PloS one. 2013; 8:e55541. [PubMed: 23383335]

Elliott KL, Houston DW, Fritzsch B. Sensory afferent segregation in three-eared frogs resemble the dominance columns observed in three-eyed frogs. Sci Rep. 2015b; 5

Ericson J, Muhr J, Placzek M, Lints T, Jessel T, Edlund T. Sonic hedgehog induces the differentiation of ventral forebrain neurons: a common signal for ventral patterning within the neural tube. Cell. 1995; 81:747–756. [PubMed: 7774016]

Fariñas I, Jones KR, Tessarollo L, Vigers AJ, Huang E, Kirstein M, De Caprona DC, Coppola V, Backus C, Reichardt LF. Spatial shaping of cochlear innervation by temporally regulated neurotrophin expression. The Journal of Neuroscience. 2001; 21:6170–6180. [PubMed: 11487640]

Forristall CA, Stellabotte F, Castillo A, Collazo A. Embryological manipulations in the developing Xenopus inner ear reveal an intrinsic role for Wnt signaling in dorsal–ventral patterning. Developmental Dynamics. 2014; 243:1262–1274. [PubMed: 24500889]

Fritzsch B. Inner ear of the coelacanth fish Latimeria has tetrapod affinities. Nature. 1987; 327:153–154. [PubMed: 22567677]

Fritzsch B. Fast axonal diffusion of 3000 molecular weight dextran amines. Journal of Neuroscience Methods. 1993; 50:95–103. [PubMed: 7506342]

Fritzsch B, Barald KF, Lomax MI. Early embryology of the vertebrate ear, Development of the auditory system. Springer. 1998:80–145.

Fritzsch B, Beisel KW, Jones K, Fariñas I, Maklad A, Lee J, Reichardt LF. Development and evolution of inner ear sensory epithelia and their innervation. Journal of Neurobiology. 2002; 53:143–156. [PubMed: 12382272]

Fritzsch B, Elliott KL. Evolution and Development of the Inner Ear Efferent System: Transforming a Motor Neuron Population to Connect to the Most Unusual Motor Protein via Ancient Nicotinic Receptors. Frontiers in Cellular Neuroscience. 2017; 11:114. [PubMed: 28484373]

Fritzsch B, Pan N, Jahan I, Duncan JS, Kopecky BJ, Elliott KL, Kersigo J, Yang T. Evolution and development of the tetrapod auditory system: an organ of Corti-centric perspective. Evolution & development. 2013; 15:63–79. [PubMed: 23331918]

Fritzsch B, Wake M. The inner ear of gymnophione amphibians and its nerve supply: a comparative study of regressive events in a complex sensory system (Amphibia, Gymnophiona). Zoomorphology. 1988; 108:201–217.

Goodman L, Model P. Superinnervation enhances the dendritic branching pattern of the Mauthner cell in the developing axolotl. The Journal of Neuroscience. 1988; 8:776–791. [PubMed: 3346721]

Groves AK, Fekete DM. Shaping sound in space: the regulation of inner ear patterning. Development. 2012; 139:245–257. [PubMed: 22186725]

Hammond KL, Loynes HE, Folarin AA, Smith J, Whitfield TT. Hedgehog signalling is required for correct anteroposterior patterning of the zebrafish otic vesicle. Development. 2003; 130:1403–1417. [PubMed: 12588855]

Harrison RG. Relations of symmetry in the developing embryo. Academy of arts and Sciences. 1945

Hartline DK, Colman DR. Rapid Conduction and the Evolution of Giant Axons and Myelinated Fibers. Current Biology. 2007; 17:R29–R35. [PubMed: 17208176]

Heretsch P, Tzagkaroulaki L, Giannis A. Modulators of the hedgehog signaling pathway. Bioorganic & Medicinal Chemistry. 2010; 18:6613–6624. [PubMed: 20708941]

Huangfu D, Anderson KV. Signaling from Smo to Ci/Gli: conservation and divergence of Hedgehog pathways from Drosophila to vertebrates. Development. 2006; 133:3–14. [PubMed: 16339192]

Hurle B, Ignatova E, Massironi SM, Mashimo T, Rios X, Thalmann I, Thalmann R, Ornitz DM. Non-syndromic vestibular disorder with otoconial agenesis in tilted/mergulhador mice caused by mutations in otopetrin 1. Human Molecular Genetics. 2003; 12:777–789. [PubMed: 12651873]

Hyman JM, Firestone AJ, Heine VM, Zhao Y, Ocasio CA, Han K, Sun M, Rack PG, Sinha S, Wu JJ. Small-molecule inhibitors reveal multiple strategies for Hedgehog pathway blockade. Proceedings of the National Academy of Sciences. 2009; 106:14132–14137.

Incardona JP, Gaffield W, Kapur RP, Roelink H. The teratogenic Veratrum alkaloid cyclopamine inhibits sonic hedgehog signal transduction. DEVELOPMENT-CAMBRIDGE. 1998; 125:3553–3562.

Jacob J, Briscoe J. Gli proteins and the control of spinal-cord patterning. EMBO reports. 2003; 4:761–765. [PubMed: 12897799]

Kaiser CL, Chapman BJ, Guidi JL, Terry CE, Mangiardi DA, Cotanche DA. Comparison of activated caspase detection methods in the gentamicin-treated chick cochlea. Hearing research. 2008; 240:1–11. [PubMed: 18487027]

Koebernick K, Hollemann T, Pieler T. A restrictive role for Hedgehog signalling during otic specification in Xenopus. Developmental Biology. 2003; 260:325–338. [PubMed: 12921735]

Kopecky B, Duncan J, Elliott K, Fritzsch B. Three-dimensional reconstructions from optical sections of thick mouse inner ears using confocal microscopy. Journal of microscopy. 2012; 248:292–298. [PubMed: 23140378]

Kopecky B, Santi P, Johnson S, Schmitz H, Fritzsch B. Conditional deletion of N-Myc disrupts neurosensory and non-sensory development of the ear. Developmental Dynamics. 2011; 240:1373–1390. [PubMed: 21448975]

Korn H, Faber DS. The Mauthner Cell Half a Century Later: A Neurobiological Model for Decision-Making? Neuron. 2005; 47:13–28. [PubMed: 15996545]

Lewis, ER., Leverenz, EL., Bialek, WS. The vertebrate inner ear. CRC PressI Llc; 1985.

Liu W, Li G, Chien JS, Raft S, Zhang H, Chiang C, Frenz DA. Sonic Hedgehog Regulates Otic Capsule Chondrogenesis and Inner Ear Development in the Mouse Embryo. Developmental Biology. 2002; 248:240–250. [PubMed: 12167401]

LoRusso PM, Rudin CM, Reddy JC, Tibes R, Weiss GJ, Borad MJ, Hann CL, Brahmer JR, Chang I, Darbonne WC. Phase I trial of hedgehog pathway inhibitor Vismodegib (GDC-0449) in patients with refractory, locally advanced or metastatic solid tumors. Clinical Cancer Research. 2011; 17:2502–2511. [PubMed: 21300762]

Martin BL, Peyrot SM, Harland RM. Hedgehog signaling regulates the amount of hypaxial muscle development during Xenopus myogenesis. Developmental biology. 2007; 304:722–734. [PubMed: 17320852]

Meinhardt, H. Seminars in cell & developmental biology. Elsevier; 2015. Models for patterning primary embryonic body axes: the role of space and time; p. 103-117.

Merchant JL. Hedgehog signalling in gut development, physiology and cancer. The Journal of physiology. 2012; 590:421–432. [PubMed: 22144577]

Morinello E, Pignatello M, Villabruna L, Goelzer P, Bürgin H. Embryofetal development study of Vismodegib, a hedgehog pathway inhibitor, in rats. Birth Defects Research Part B: Developmental and Reproductive Toxicology. 2014; 101:135–143. [PubMed: 24692404]

Murone M, Rosenthal A, de Sauvage FJ. Sonic hedgehog signaling by the patched–smoothened receptor complex. Current Biology. 1999; 9:76–84. [PubMed: 10021362]

Nagase T, Nagase M, Osumi N, Fukuda S, Nakamura S, Ohsaki K, Harii K, Asato H, Yoshimura K. Craniofacial anomalies of the cultured mouse embryo induced by inhibition of sonic hedgehog signaling: an animal model of holoprosencephaly. Journal of Craniofacial Surgery. 2005; 16:80–88. [PubMed: 15699650]

Nichols DH, Pauley S, Jahan I, Beisel KW, Millen KJ, Fritzsch B. Lmx1a is required for segregation of sensory epithelia and normal ear histogenesis and morphogenesis. Cell and tissue research. 2008; 334:339–358. [PubMed: 18985389]

Nieuwkoop PD, Faber J. Normal table of Xenopus laevis (Daudin). A systematical and chronological survey of the development from the fertilized egg till the end of metamorphosis. Normal table of Xenopus laevis (Daudin). A systematical and chronological survey of the development from the fertilized egg till the end of metamorphosis. 1956:22.

Pauley S, Lai E, Fritzsch B. Foxg1 is required for morphogenesis and histogenesis of the mammalian inner ear. Developmental Dynamics. 2006; 235:2470–2482. [PubMed: 16691564]

Peukert S, Jain RK, Geisser A, Sun Y, Zhang R, Bourret A, Carlson A, DaSilva J, Ramamurthy A, Kelleher JF. Identification and structure–activity relationships of ortho-biphenyl carboxamides as potent Smoothened antagonists inhibiting the Hedgehog signaling pathway. Bioorganic & Medicinal Chemistry Letters. 2009; 19:328–331. [PubMed: 19091559]

Piatt J. The influence of VIIth and VIIIth cranial nerve roots upon the differentiation of Mauthner's cell in Ambystoma. Developmental Biology. 1969; 19:608–616. [PubMed: 5772672]

Riccomagno MM, Martinu L, Mulheisen M, Wu DK, Epstein DJ. Specification of the mammalian cochlea is dependent on Sonic hedgehog. Genes & development. 2002; 16:2365–2378. [PubMed: 12231626]

Riccomagno MM, Takada S, Epstein DJ. Wnt-dependent regulation of inner ear morphogenesis is balanced by the opposing and supporting roles of Shh. Genes & development. 2005; 19:1612–1623. [PubMed: 15961523]

Rudin CM. Vismodegib. Clinical Cancer Research. 2012; 18:3218–3222. [PubMed: 22679179]

Scales SJ, de Sauvage FJ. Mechanisms of Hedgehog pathway activation in cancer and implications for therapy. Trends in Pharmacological Sciences. 2009; 30:303–312. [PubMed: 19443052]

Sharpe HJ, Wang W, Hannoush RN, de Sauvage FJ. Regulation of the oncoprotein Smoothened by small molecules. Nature chemical biology. 2015; 11:246–255. [PubMed: 25785427]

Shimizu Y, Ishii T, Ogawa K, Sasaki S, Matsui H, Nakayama M. Biochemical characterization of smoothened receptor antagonists by binding kinetics against drug-resistant mutant. European Journal of Pharmacology. 2015; 764:220–227. [PubMed: 26048307]

Villavicencio EH, Walterhouse DO, Iannaccone PM. The sonic hedgehog–patched–gli pathway in human development and disease. The American Journal of Human Genetics. 2000; 67:1047–1054. [PubMed: 11001584]

Waldman EH, Castillo A, Collazo A. Ablation studies on the developing inner ear reveal a propensity for mirror duplications. Developmental Dynamics. 2007; 236:1237–1248. [PubMed: 17394250]

Whitfield TT, Hammond KL. Axial patterning in the developing vertebrate inner ear. International Journal of Developmental Biology. 2007; 51:507–520. [PubMed: 17891713]

Wu DK, Kelley MW. Molecular mechanisms of inner ear development. Cold Spring Harbor perspectives in biology. 2012; 4:a008409. [PubMed: 22855724]

Yang ZJ, Ellis T, Markant SL, Read TA, Kessler JD, Bourboulas M, Schüller U, Machold R, Fishell G, Rowitch DH. Medulloblastoma can be initiated by deletion of Patched in lineage-restricted progenitors or stem cells. Cancer cell. 2008; 14:135–145. [PubMed: 18691548]

Yauch RL, Dijkgraaf GJ, Alicke B, Januario T, Ahn CP, Holcomb T, Pujara K, Stinson J, Callahan CA, Tang T. Smoothened mutation confers resistance to a Hedgehog pathway inhibitor in medulloblastoma. science. 2009; 326:572–574. [PubMed: 19726788]

Yntema, C. The symmetry of ears induced from disharmonic ectoderm, ANATOMICAL RECORD WILEY-LISS DIV. JOHN WILEY & SONS INC; 605 THIRD AVE, NEW YORK, NY 10158-0012: 1948. p. 727-727.

Yu J, Carroll TJ, McMahon AP. Sonic hedgehog regulates proliferation and differentiation of mesenchymal cells in the mouse metanephric kidney. Development. 2002; 129:5301–5312. [PubMed: 12399320]

Zarei K, Elliott KL, Zarei S, Fritzsch B, Buchholz J. A Method for Detailed Movement Pattern Analysis of Tadpole Startle Response. Journal of the Experimental Analysis of Behavior. 2017

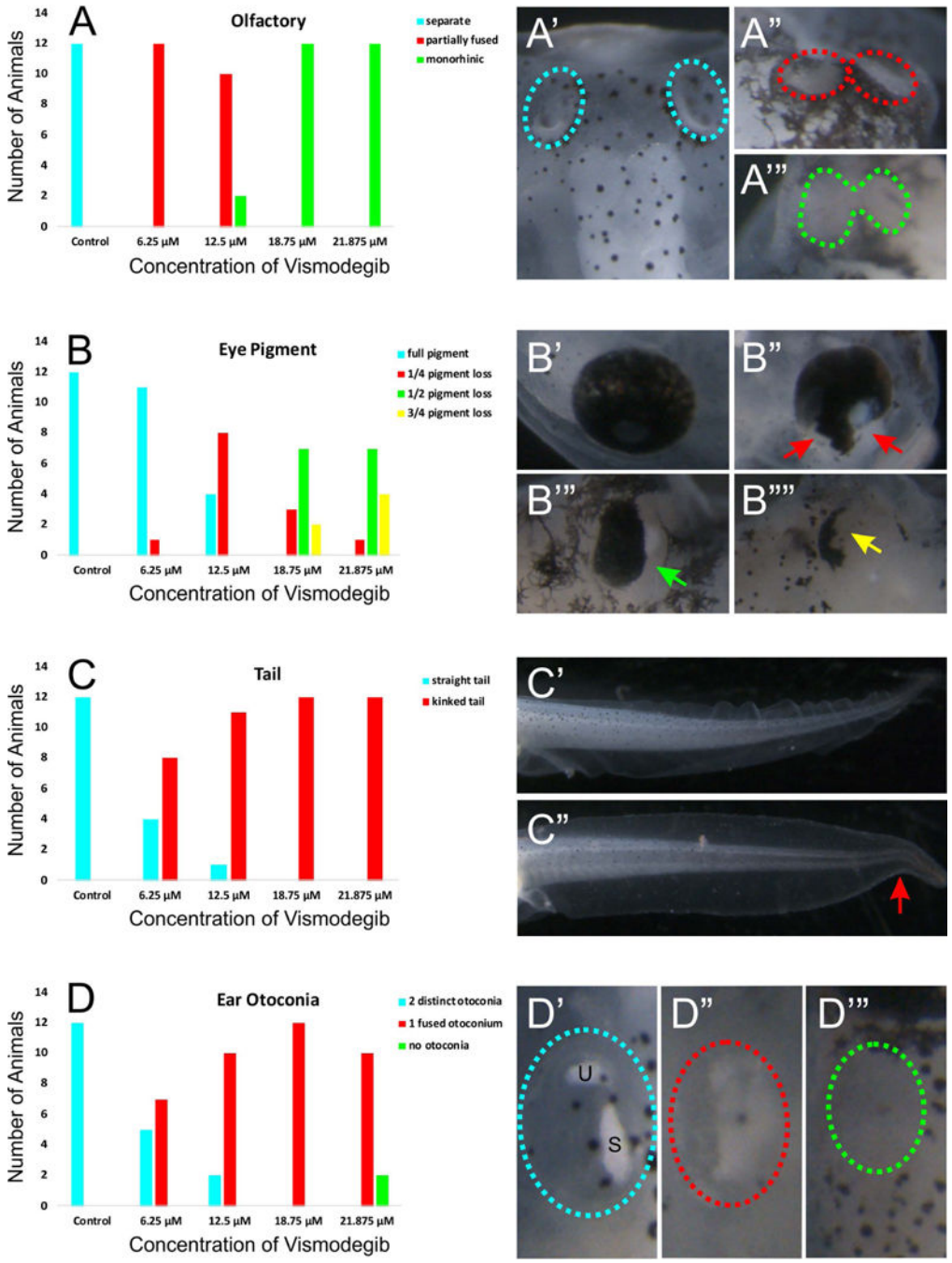

Figure 1. Varied concentrations of Vismodegib result in a dose-dependent effect on phenotypic changes

A) Control tadpoles display two distinct olfactory groves (A'). However, increasing Vismodegib concentration results in an increasing tendency towards complete fusion of the two groves (A"-A"'). Animals treated with 6.25 µM Vismodegib exhibited partially fused olfactory epithelia (A"). By 18.75 µM of Vismodegib, all animals exhibited complete fusion of the olfactory epithelia (A"'). **B)** Eye pigmentation was also affected following treatment with Vismodegib. Compared to control animals which exhibited full eye pigmentation (B'),

animals treated with 6.25 μM Vismodegib began to lose eye pigmentation in the ventral part of the eye (B”). This loss of ventral eye pigmentation was more profound in animals treated with 12.5 μM Vismodegib. About half of animals treated with 18.75 μM had pigment loss in half of the ear (B”’). In a couple animals treated with 18.75 μM and about one third of animals treated with 21.875 μM Vismodegib had very little eye pigment remaining (B””). **C)** Tail development was variably affected as a result of reduced Shh signaling. Animals treated with 12.5 μM, 18.75 μM, and 21.875 μM Vismodegib exhibited a kink at the caudal portion of their tails (C”) compared to the straight tail of control animals (C’). At 6.25 μM Vismodegib, fewer animals exhibited kinked tails. **D)** Aberrations in otoconia development were also evident with Vismodegib treatment. Control tadpoles had two distinct otoconia (D’). Some animals treated with 6.25 μM Vismodegib, most animals treated with 12.5 μM Vismodegib, and all animals treated with 18.75 μM Vismodegib had a single otoconia mass (D”). A couple animals treated with 21.875 μM lacked otoconia formation altogether (D”’), whereas the rest had one otoconia mass (D”).

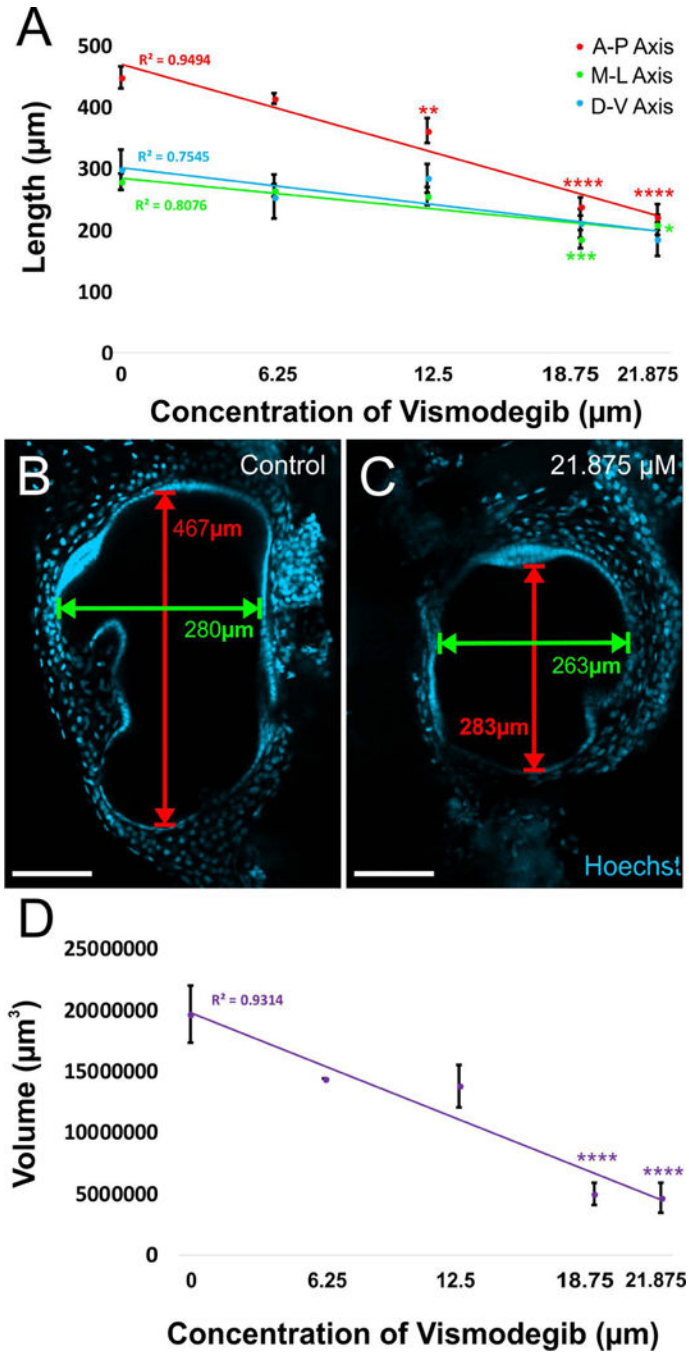

Figure 2. Reduction in ear length along both the anteroposterior and mediolateral axes in Vismodegib treated tadpoles

A) The reduction in ear length along anteroposterior, mediolateral, and dorsoventral axes followed a linear dose response curve. This decrease in ear size was more profound along the anteroposterior dimension of the ear compared to the mediolateral or dorsoventral dimension of the ear. While ears from animals treated with 12.5 µM and greater doses of Vismodegib were significantly reduced in length along the anteroposterior axis from controls, only 18.75 µM and 21.875 µM Vismodegib-treated animals were significantly reduced along the mediolateral axis from controls. The reduction in length along the

anteroposterior axis at the highest dose of Vismodegib was approximately 2-fold, whereas along the mediolateral axis, it was only approximately 1.3-fold. **B)** Illustration of lengths measured along the anteroposterior axis and mediolateral axis in the ear of a stage 46 control tadpole. **C)** Illustration of lengths measured along the anteroposterior axis and mediolateral axis in the ear of a stage 46 tadpole treated with 21.875 μM Vismodegib. Scale bars represent 100μm. **D)** The reduction in approximate volume as calculated from the anteroposterior, mediolateral, and dorsoventral lengths from each ear followed a linear dose response curve. The volumes of animals treated with 18.75 μM and 21.875 μM Vismodegib were significantly reduced to approximately $1/4^{th}$ the volume of controls. * $p<0.05$, ** $p<0.01$, ***$P<0.001$, ****$p<0.0001$ (ANOVA).

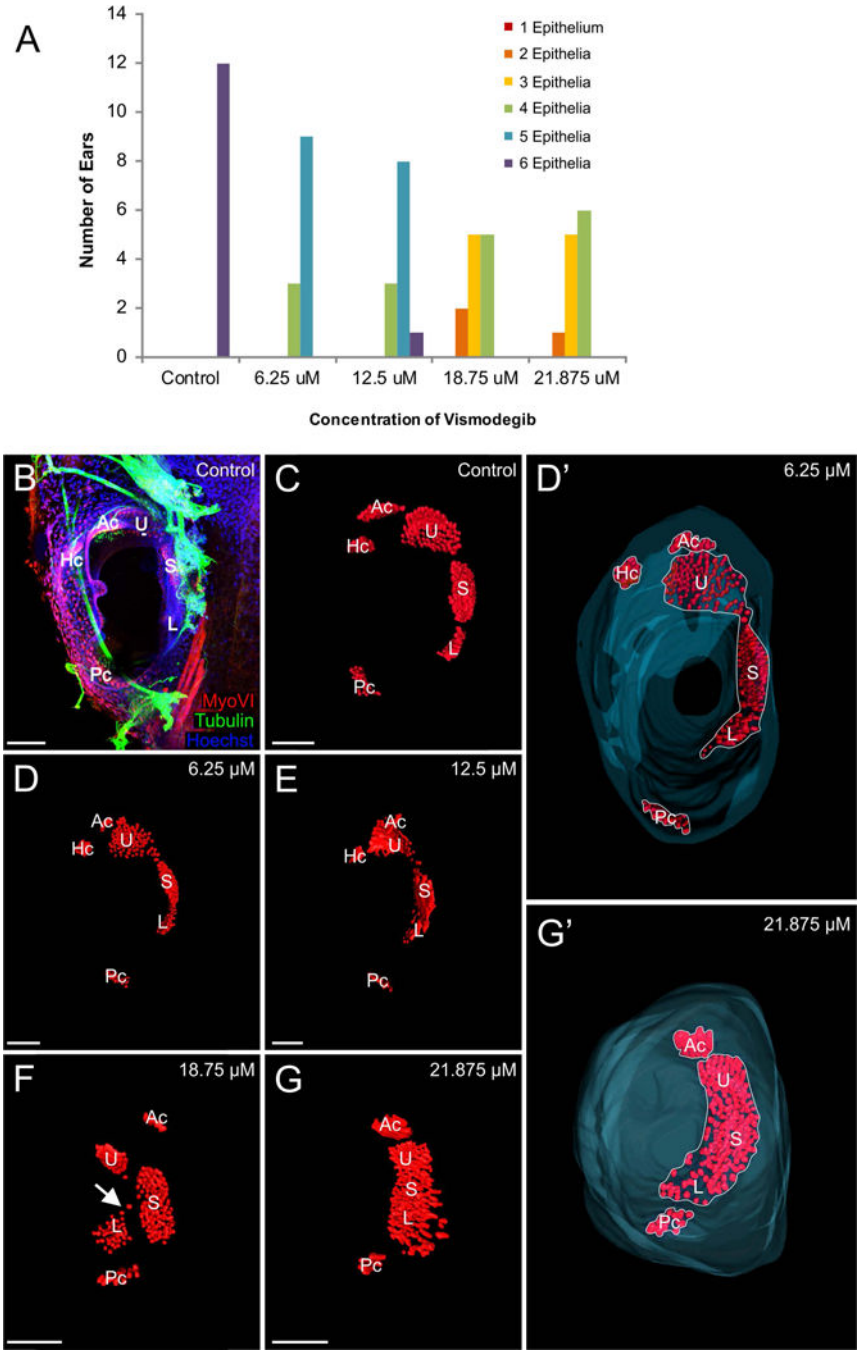

Figure 3. Effect of Vismodegib on inner ear sensory epithelia development

A) Animals treated with Vismodegib exhibited a dose-dependent reduction in sensory epithelia development. **B)** Immunohistochemistry using antibodies against Tubulin (green) and MyoVI (red) to label neurons and hair cells, respectively. Shown here is a control ear. **C)** 3D reconstruction of hair cells shows that in control animals, there are six distinct sensory epithelia. **D-D')** 3D reconstruction of hair cells from an animal treated with 6.25 µM Vismodegib showing four distinct sensory epithelia. **E)** 3D reconstruction of hair cells from an animal treated with 12.5 µM Vismodegib showing four distinct sensory epithelia. **F)** 3D

reconstruction of hair cells from an animal treated with 18.75 μM Vismodegib showing four distinct sensory epithelia. Sensory epithelial patches were sometimes connected by a few hair cells in a "bridge" (arrow). **G-G')** 3D reconstruction of hair cells from an animal treated with 21.875 μM Vismodegib showing three distinct epithelia. In D' and G' Hoechst staining was used to 3D reconstruct the inner boundary of the ears, shown in blue. Note the reduction in distinct epithelia (compare outlines in D',G') exceeds the reduction in hair cells. Ac anterior canal crista, Hc horizontal canal crista, Pc posterior canal crista, U utricle, S saccule, L lagena. Scale bars represent 100μm.

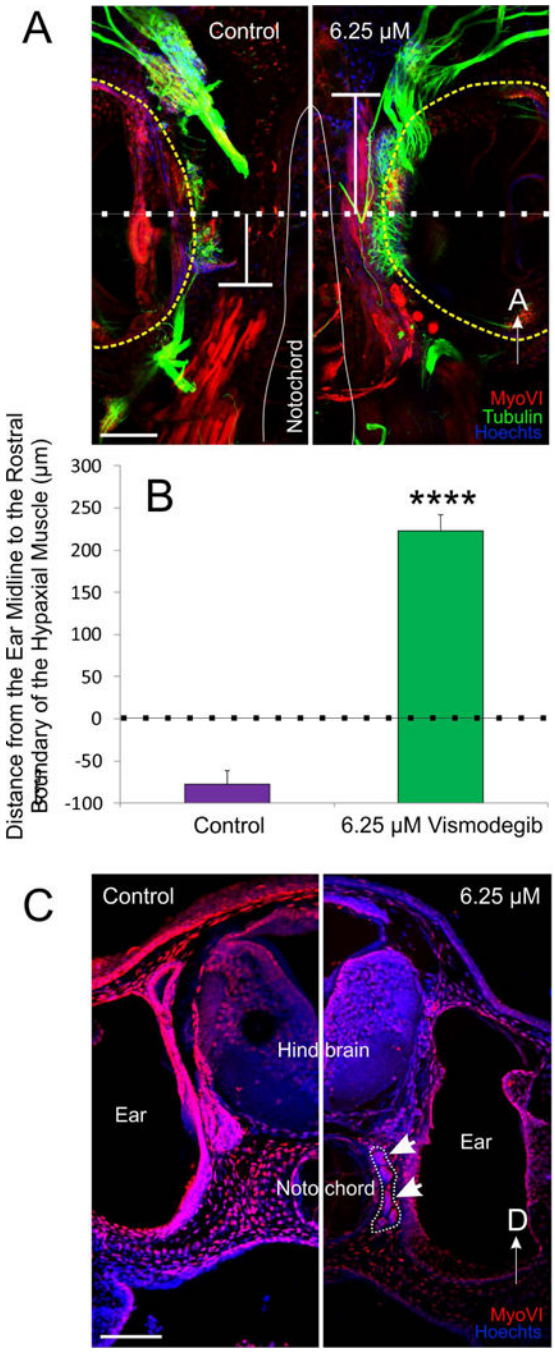

Figure 4. Rostral expansion of hypaxial muscle fibers following Vismodegib treatment

A) The distance from the ear midline from the rostral boundary of the somites was calculated from animals immunostained with antibodies against tubulin (green), MyoVI (red) and counterstained with Hoechsts to label neurons, hair cells and muscle tissue, and nuclei, respectively. A line was drawn through the midline of the ear (dotted line), calculated from the anteroposterior diameter of the ear. From that line, the distance to the rostral boundary of the somites was determined (T-shaped line). Positive values were assigned for distances rostral to the midline and negative values for distances caudal to the midline. **B)**

Means plus or minus standard errors of the mean for both controls and animals treated with 6.25 μM Vismodegib calculated using the method from (A). ****p<0.0001 **C)** Coronal section showing that hypaxial muscle fibers (outlined and arrows) expanded between the brain and the ear in animals treated with 6.25 μM Vismodegib. Scale bars represent 100μm.

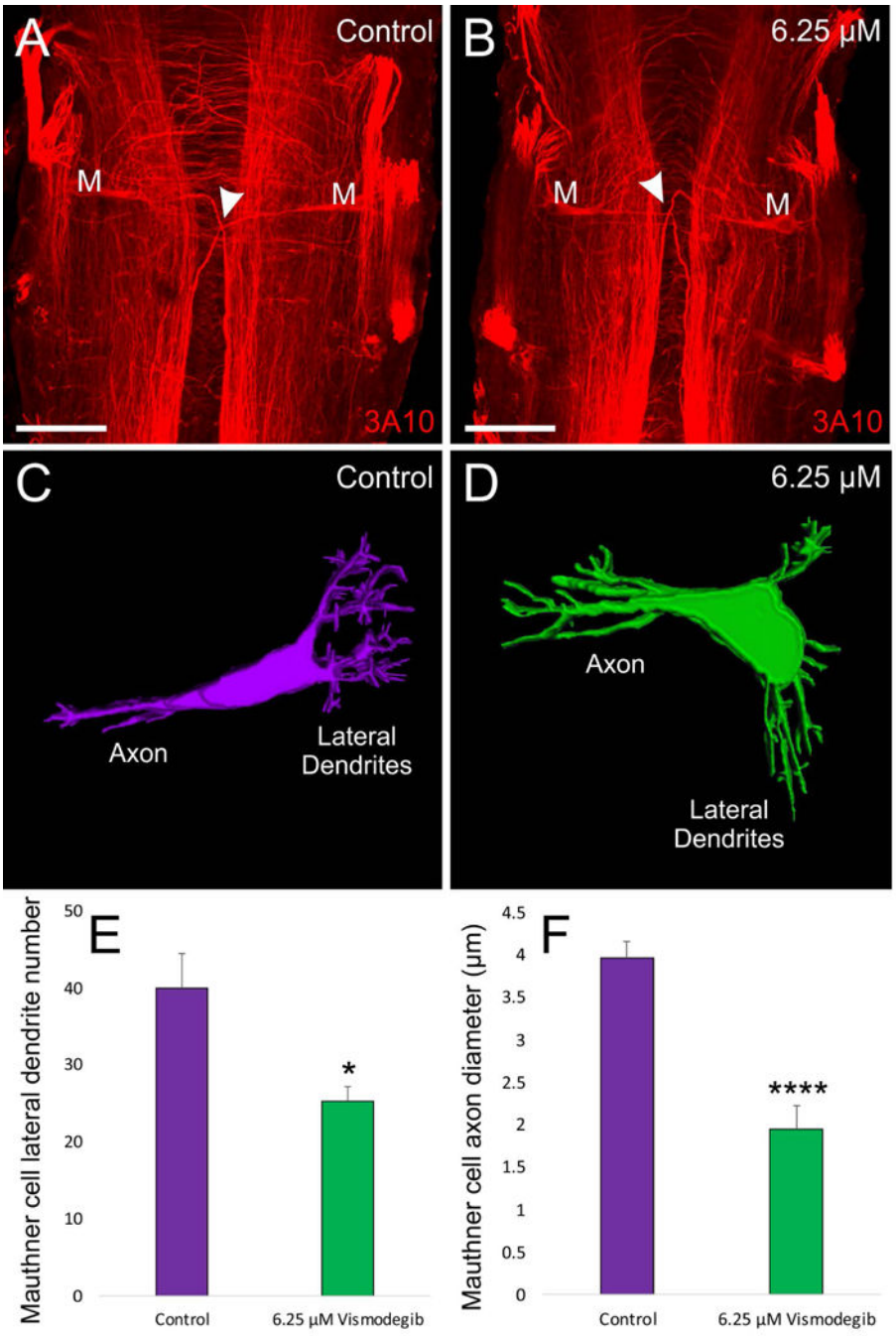

Figure 5. Effect of Vismodegib treatment on Mauthner Cell Development

A) 3A10 antibody labeling of a pair of Mauthner cells from a control *Xenopus*.-**B)** 3A10 antibody labeling of a pair of Mauthner cells from an animal treated with 6.25 µM Vismodegib. Arrowheads for A and B indicate axon crossing at the midline. **C)** 3D reconstruction of a control Mauthner cell from dextran amine labeling **D)** 3D reconstruction of a Mauthner cell from an animal treated with 6.25 µM Vismodegib. **E)** Shh inhibition results in a significant reduction in the degree of branching of the Mauthner cell in 6.25 µM Vismodegib-treated animals (n = 4) compared to control animals (n = 4). **F)** Shh inhibition

results in an approximately two-fold reduction in axonal diameter of the Mauthner cell in 6.25 μM Vismodegib-treated animals (n = 3) compared to control animals (n = 5). Scale bars represent 100 μm.* $p<0.05$, ****$p<0.0001$.

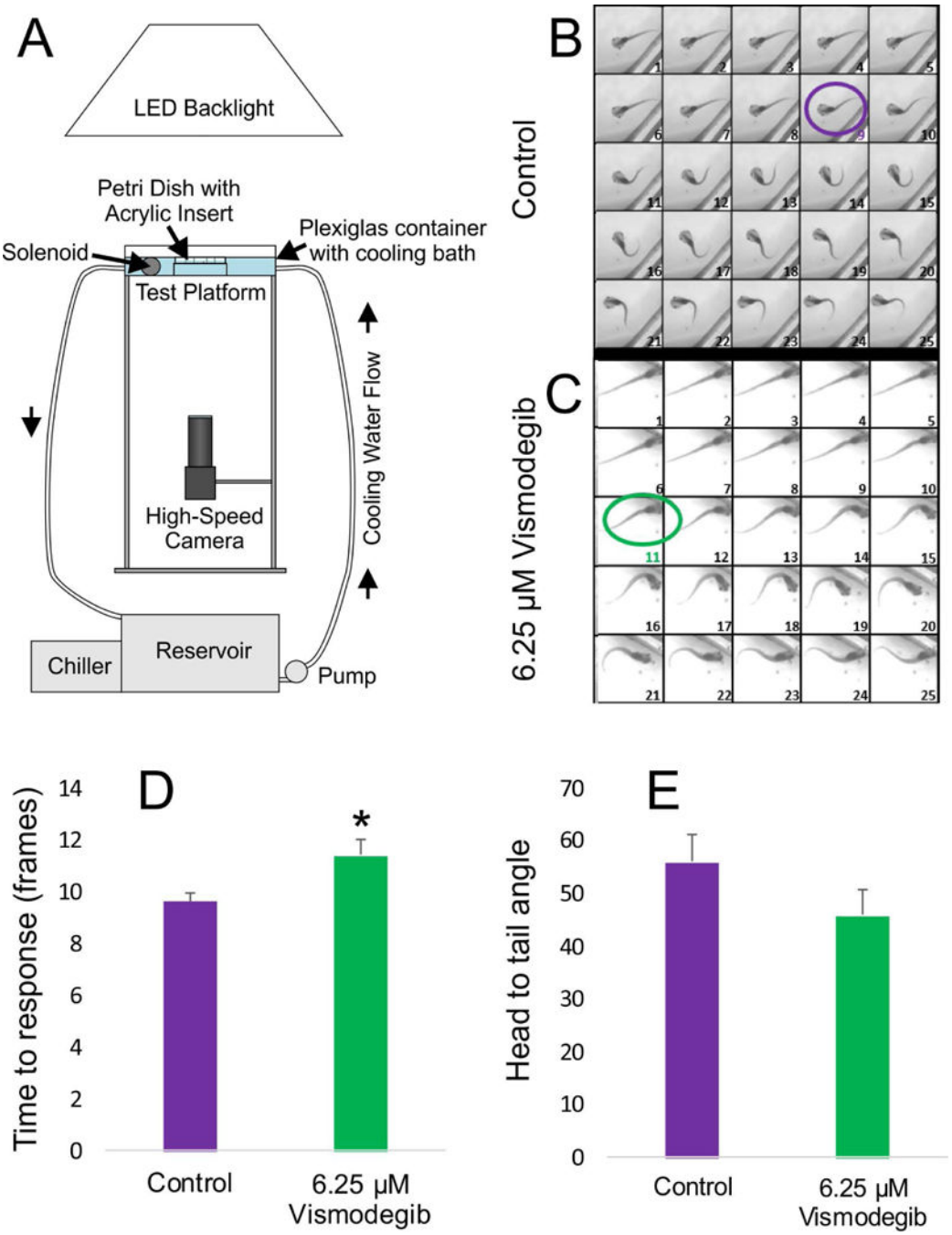

Figure 6. Impact of Vismodegib treatement on tadpole swimming behavior

A) Schematic of imaging apparatus utilized for recording tadpole swimming behavior and the C-start response following a controlled perturbation, as described by Zarei et al (2017). **B–C)** Images of the first 25 frames captured following initiation of the stimulus for both control animals (B) and animals treated with 6.25 µM Vismodegib (C). Control animals on average took 9 frames to elicit the C-start response (purple circle), whereas animals treated with 6.25 µM Vismodegib took 11 frames (green circle), based on the criteria described in Zarei et al. (2017). **D)** The time to elicit a C-start response was significantly longer in

animals treated with 6.25 μM Vismodegib than in control animals. * $p<0.05$. **E)** Though not significant, the maximal flexion in in animals treated with 6.25 μM Vismodegib was, on average, tighter than that of control animals, resulting in an atypical U-shaped configuration instead of the normal C-shaped configuration.

Table 1

Sensory epithelia phenotypes following treatment with vismodegib. Numbers indicate the number of ears with each described condition. Ears may be included in more than one condition. Total number of ears examined were 12 per treatment (6 animals).

Vismodegib Concentration	Number with Fused Saccule- Lagena	Number with Fused Utricle-Saccule-Lagena	Number with Absent Horizontal Canals	Number with Absent Anterior Canals
Control	0	0	0	0
6.25 μM	12	1	2	0
12.5 μM	11	4	1	0
18.75 μM	12	10	8	2
21.875 μM	12	12	7	1